Role of bound pairs in the optical properties of highly excited semiconductors: A self-consistent ladder approximation approach

C. Piermarocchi
Department of Physics, University of California San Diego, La Jolla, California 92093-0319

F. Tassone
Scuola Internazionale Superiore di Studi Avanzati, via Beirut 4, I-34014 Trieste, Italy

(Received 12 September 2000; revised manuscript received 1 February 2001; published 4 June 2001)

The presence of bound pairs (excitons) in a low-temperature electron-hole plasma is accounted for by including correlation between fermions at the ladder level. Using a simplified one-dimensional model with on-site Coulomb interaction, we calculate the one-particle self-energies, chemical potential, and optical response. The results are compared to those obtained in the Born approximation, which does not account for bound pairs. In the self-consistent ladder approximation the self-energy and spectral function show a characteristic correlation peak at the exciton energy for low temperature and density. In this regime the Born approximation overestimates the chemical potential. Provided the appropriate vertex correction in the interaction with the photon is included, both ladder and Born approximations reproduce the excitonic and free pair optical absorption at low density, and the disappearance of the exciton absorption peak at larger density. However, line shapes and energy shifts of the absorption and photoluminescence peaks with density are drastically different. In particular, the photoluminescence emission peak is much more stable in the ladder approximation. Moreover, even though at low temperature and density a sizable optical gain is produced in both approximations just below the excitonic peak, this gain shows unphysical features in the Born approximation.

DOI: 10.1103/PhysRevB.63.245308 PACS number(s): 78.55.−m, 71.35.Ee

I. INTRODUCTION

The binding of a gas of oppositely charged fermions leading to a gas of bosons has a fundamental interest in condensed matter physics, in problems ranging from the state of hydrogen to the nature of the electron-hole plasma in Si and Ge. This pairing takes its origin from the Coulomb correlation between the charged fermions, and strongly affects the statistical and thermodynamic properties of these systems. In semiconductor physics, the role of the Coulomb correlation and pairing in the description of the electron-hole plasma in Si and Ge has been extensively investigated. Refined descriptions of both the ground state and the thermodynamic properties of this system have been developed over the past 30 years. In particular, an excitonic insulator ground state was first proposed and then shown to be less stable than a simpler electron-hole liquid in Si and Ge, due to band-structure effects.[1] Thermodynamics of the electron-hole gas in simpler crystals was also addressed by Haug[2] and Zhu *et al.*[3] aiming at deriving a complete phase diagram from variational approaches.

In this paper we will deal with direct gap semiconductors and we will discuss the thermodynamics of the photoexcited electron and holes at quasithermal equilibrium. Our main concern is to determine how the inclusion of pairing effects in the theoretical description, as done for the systems mentioned above, can affect predictions on the shape of optical spectra. In the optical properties of semiconductors, the effect of the Coulomb electron-hole correlation comes into play to explain the characteristic excitonic absorption and emission. These excitonic features can be described by including vertex corrections in the interaction of the electron-hole pair with the photon.[4] In particular, excitonic absorption is found in an empty crystal, when a background electron-hole plasma is absent. However, when carriers are electrically or optically injected, they reach quasithermal equilibrium through scattering, and a background electron-hole plasma is eventually formed. In this typical situation the absorption is modified, and spontaneous emission (photoluminescence) also takes place. Absorption and emission give valuable information about the state of the plasma, but a theory describing both the thermodynamics and optical properties of the plasma is required in order to extract this information. Semiconductor Bloch equations and their evolutions are certainly among the most known and used theories for this purpose.[5] In these theories, the electron-hole plasma has been originally treated at the Hartree-Fock level,[6] and eventually screening of the Coulomb interaction was also included at various levels of approximation.[5] However, none of these refinements accounts for the existence of bound excitons in the plasma. This is certainly a weak point at low temperatures, when simple thermodynamic arguments show that condensation of the electron-hole gas into a gas of bound electron-hole pairs is favorable in a wide range of densities.

In the following sections we will show the relevant changes in the optical properties of the semiconductor when the existence of excitons at low temperatures is taken into account. Our purpose is qualitative, but we can still gain solid understanding of the underlying physics. We thus consider an accurately solvable model, where the system is one-dimensional, the Coulomb interaction is on-site, and electron and holes are spin-polarized. Excitonic correlation is also expected to be stronger in one dimension than higher dimen-

sions. Moreover, for the single-pair problem, exactly a single bound state is obtained with the on-site interaction. In our description of the electron-hole plasma, we either include carrier scattering at the Born level, which does not describe bound pairs in the plasma, or we include enough correlation so as to describe the pairing into bound states. For this purpose, ladder diagrams in the electron-hole scattering kernel[7–9] are included, and the electron and hole self-energies calculated with it.[10] The resulting Dyson equations for the Green functions are solved self-consistently. The approximation is therefore called the self-consistent ladder approximation (SCLA). Screening is expected to be weak in one dimension,[11] due to reduced screening phase space, and we neglect it altogether. We remark that in the SCLA we calculate the single-particle propagators and self-energies only; thus in this sense, the theory remains purely fermionic. We do not map the model onto bound and unbound states at any time. However, it is possible to show analytically that at low temperatures and densities, a bosonic gas of excitons is effectively described, and that self-consistency effectively introduces scattering between these excitons. When this analogy is extended to larger densities and temperatures, where bound and free carriers are expected to coexist, we understand that self-consistency also accounts for multiple exciton–free-carrier and free-carrier-free-carrier scattering. Thus, a large amount of correlation, well beyond that described in simpler Born approximations, is included in the SCLA. We remark that we also assume quasithermal equilibrium in the electron-hole gas, which is well justified as the characteristic radiative recombination (several hundreds of picoseconds) is much slower than the typical scattering time in the density range considered. We finally show how to correctly calculate photon absorption and emission [photoluminescence (PL)] in a conserving sense, i.e., respecting *f*-sum rules. We only neglect polaritonic effects, which are very weak in one dimension.[12]

Within the considered models, we highlight the following trends in optical and thermodynamic properties. First, Born approximations overestimate the chemical potential at low temperatures when a consistent fraction of pairs is bound into excitons. Second, energetic stability of the excitonic emission peak as a function of density is better described in the SCLA, even well beyond disappearance of excitonic absorption peak at large excitation densities. Third, the large excitonic *gain* at densities just below those where excitonic absorption disappears is clearly incorrectly described in simpler Born approximations. As these trends have a clear physical origin, they are expected to hold qualitatively even when more realistic interaction potentials (eventually including screening) are considered. These results signal the necessity of an adequate description of the excited semiconductor in the low-temperature region. For example, the current description of the electron-hole plasma in the semiconductor Bloch equations is clearly insufficient to address excitonic (inversionless) lasing.

The paper is organized as follows. In Sec. II we introduce and explain how to implement the self-consistent ladder approximation, the Markov-Born approximation, and the self-consistent Born approximation. Single-particle properties are analyzed in Sec. III, where we show the appearance of excitonic correlation structures in the electron and hole spectral functions. Chemical potentials and self-energies are then compared. In Sec. IV we analytically show how the SCLA at low temperature and density describes an interacting exciton gas. Optical properties of a semiconductor quantum wire are calculated in Sec. V for the three approximations. Absorption and emission as functions of density are also presented and discussed in this section. Conclusions are drawn is Sec. VI.

II. BORN AND SELF-CONSISTENT LADDER APPROXIMATIONS

In this section we introduce the SCLA, the simpler Markov-Born approximation (MBA), and self-consistent Born approximation (SCBA). We assume thermal equilibrium in the electron-hole plasma, but, in order to avoid analytic continuation problems, we do not resort to the Matsubara Green's function technique,[13] which becomes numerically delicate when the spectral function shows a large number of poles. Instead, we work directly in the real time/frequency space. This has the additional advantage that the approach can be readily extended to nonequilibrium conditions.[14] We thus consider four single-particle Green's functions:[15] the retarded, advanced, lesser, and greater Green's functions defined as

$$G^{+}(1,2) = -i\,\theta(t_1 - t_2)\langle T[c(1)c^{\dagger}(2)]_{+}\rangle, \tag{1a}$$

$$G^{-}(1,2) = i\,\theta(t_2 - t_1)\langle T[c(1)c^{\dagger}(2)]_{+}\rangle, \tag{1b}$$

$$G^{<}(1,2) = i\langle c^{\dagger}(2)c(1)\rangle, \tag{1c}$$

$$G^{>}(1,2) = -i\langle c(1)c^{\dagger}(2)\rangle. \tag{1d}$$

Here T is the time ordering operator, and $1=(x_1,t_1,\sigma_1)$, where x_1 is the position, t_1 the time, and σ_1 is the spin index. $c(1)$ is the electron annihilation operator and $[\,]_+$ is the anticommutator. Similar expressions for the hole Green's functions hold, with $d(1)$ and $d^{\dagger}(1)$ the hole annihilation and creation, respectively. Only two of the four functions above are independent, and in particular, we will consider the retarded and lesser (or correlation) functions. Formally, a single Green's function $G(x_1,\tau_1,x_2,\tau_2)$ may be introduced for compactness of notation, with τ_1 and τ_2 defined on the Keldysh contour. Following simple rules, any equation with times defined on the Keldysh contour can be written in a set of equations defined on the ordinary time axis for the four Green functions above (see, for instance, Ref. 15).

The statistical averages are done in the macrocanonical ensemble: $\langle\cdots\rangle = \mathrm{Tr}\{\rho\cdots\}$, with $\rho = e^{-\beta(H-\mu_e N_e-\mu_h N_h)}/\mathrm{Tr}\{e^{-\beta(H-\mu_e N_e-\mu_h N_h)}\}$. Here $\beta = 1/T$ and H is the total Hamiltonian of the interacting electron-hole system. In principle, electrons and holes have independent chemical potentials and densities. However, we are interested in the description of a laser-excited semiconductor where the density of electrons and holes is the same and the charge is balanced. We will also assume that the temperature of the two components of the interacting gas is the same. In fact, after excita-

tion, thermalization of carriers is mainly driven by exchange of energy with the phonon thermal bath, which, at equilibrium, leads to $T_e=T_h=T$. Moreover, for simplicity we consider the same electron and hole masses, giving $\mu_e=\mu_h=\mu$ and the same Green's functions and self-energies. Extension of the theory to different masses is straightforward. Finally, the Green's functions above depend only on the time difference t_2-t_1 as the system is stationary and on the relative distance x_2-x_1 as the system is homogeneous.

In this thermal regime, the retarded and lesser Green functions defined above are also related by the Kubo-Martin-Schwinger relations[16]

$$G^<(k,\omega)=-2\,\mathrm{Im}[G^+(k,\omega)]f(\omega-\mu), \tag{2a}$$

$$G^>(k,\omega)=2\,\mathrm{Im}[G^+(k,\omega)][1-f(\omega-\mu)], \tag{2b}$$

where we considered the Fourier transforms with respect to the relative time t_1-t_2 and with respect to the relative position x_1-x_2. The function $f(\omega)=[\exp(\omega/T)+1]^{-1}$ is the Fermi function. In the stationary case $G^+(k,\omega,\sigma)=G^-{}^*(k,\omega,\sigma)$ contain the information on the spectral properties of the quasiparticles, given by the one particle spectral function $A(k,\omega,\sigma)=-2\,\mathrm{Im}[G^+(k,\omega,\sigma)]$. The correlation functions instead contain information on the quasiparticle occupation number $G^<(k,t_1=t_2=t,\sigma)=N(k,t,\sigma)$ and $G^>(k,t_1=t_2=t,\sigma)=1-N(k,t,\sigma)$ where $N(k,t\sigma)$ are the occupation numbers.

The on-site Coulomb interaction reads

$$V(x)=\pm a\,\delta(x), \tag{3}$$

and the potential is repulsive for electron-electron and hole-hole interactions and attractive for the electron-hole interaction. An attractive δ-function-like potential between the electrons and the holes gives one bound state only for the pair problem, and a can be chosen such to reproduce the exciton binding energy measured in the limit of low density. The constant a has the dimensions of (energy)$\times$(length), the exciton Bohr radius is given by $a_B=\hbar^2/(ma)$ and the exciton binding energy is $E_b=ma^2/2\hbar^2$, where m is the reduced mass of the electron-hole system. We will use the units $\hbar=a=m=1$ throughout the paper. In these units $a_B=1$ and $E_b=0.5$. We remind the reader that typical values for semiconductor quantum wires are $a_B=10^{-6}$ cm and $E_b=10$ meV.[17] With the above effective potential of Eq. (3) the interaction Hamiltonian is

$$\begin{aligned} H_C=&\frac{1}{2}\sum_1 c^\dagger(1)c^\dagger(1')c(1')c(1)\\ &+\frac{1}{2}\sum_1 d^\dagger(1)d^\dagger(1')d(1')d(1)\\ &-\sum_1 c^\dagger(1)d^\dagger(1')c(1)d(1'). \end{aligned} \tag{4}$$

Here $1'=(x_1,t_1,\sigma'\neq\sigma)$ for the electron-electron and hole-hole interactions, while $1'=(x_1,t_1,\sigma')$ for the electron-hole interaction, as due to the fermionic nature of the carriers, only interaction with opposite spin is allowed in the intraband term for a contact potential. In the following, we assume a spin-polarized system of electrons and holes, so that we keep only the last term describing the electron-hole interaction in the Hamiltonian (4). Generalization to both spins is straightforward.

The Dyson equation for the single particle $G(1,2)$ propagators read

$$G(1,2)=G_0(1,2)+\int d\bar{3}d\bar{4}G_0(1,\bar{3})\Sigma(\bar{3},\bar{4})G(\bar{4},2), \tag{5}$$

where time integrations are over the Keldysh contour. G_0 is the free propagator. The functional dependence of the self-energy Σ on the single-particle Green's functions determines the degree of approximation. In particular, it can be expressed through an electron-hole scattering kernel $T(1,2;1',2')$:

$$\Sigma(1,2)=i\int d\bar{1}'d\bar{2}'T(1,\bar{1}';2,\bar{2}')G(\bar{2}',\bar{1}'). \tag{6}$$

In the Born approximation,

$$T(1,1';2,2')=V(1,1')+V(1,1')iG(1,2)G(1',2')V(2,2'), \tag{7}$$

where $V(1,1')=V(x_1-x_{1'})\delta(t_1,t_{1'})$, and $\delta(\tau,\tau')$ is the Dirac δ function extended on the Keldysh contour. The self-energy $\Sigma(k,\omega)$ can be calculated at the single-particle pole $\omega=k^2/4$. In this case we are neglecting memory terms in the scattering and thus using a Markov approximation; this corresponds to the MBA and is a non-self-consistent approximation. In the SCBA, the same scattering kernel of Eq. (7) is used, but the full energy-dependent structure of the resulting self-energy given in Eq. (6) is used in the Dyson equations, Eq. (5). The problem is then solved self-consistently, as explained later. In this case, memory effects, beyond the Markov approximation, are also included. In the SCLA, the kernel $T(1,1';2,2')$ is the solution of the Bethe-Salpeter equations in the ladder approximation, which for a generic potential reads

$$\begin{aligned} T(1,1';2,2')=&V(1,1')+\int d\bar{3}d\bar{3}'V(1,1')iG(1,\bar{3})\\ &\times G(1',\bar{3}')T(\bar{3},\bar{3}';2,2'). \end{aligned} \tag{8}$$

For a δ-like potential, $V(1,1')=-\delta(1,1')$ and T depends only on $2-1$. The reduced equation reads:

$$T(1;2)=-1-i\int d\bar{3}G(1,\bar{3})G(1,\bar{3})T(\bar{3};2). \tag{9}$$

Equations (5), (6), and (8) are schematically represented in Fig. 1 for both the SCBA and the SCLA.

In the self-consistent approximation we solve Eqs. (5) and (6) self-consistently with the scattering kernels given by Eq. (7) or (8) in the Born or SCLA case, respectively. We explain in detail how numerical self-consistency for a fixed temperature and chemical potential μ has been implemented.

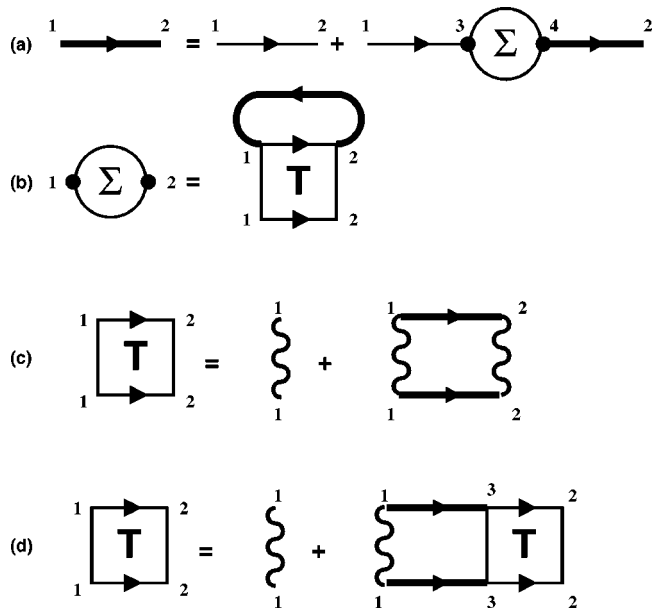

FIG. 1. (a) The Dyson equation: thick lines are the dressed one-particle Green function and thin lines the bare ones. (b) The self-energy with the scattering kernel $T(1;2)$, for the on-site Coulomb potential. (c) The scattering kernel $T(1;2)$ for the Born approximations. (d) The scattering kernel $T(1;2)$ in the ladder approximation, given by the Bethe-Salpeter equation.

(i) We start with $G^+(k,\omega)$ of the form $G^+{}_0=(\omega-k^2/4+i\gamma)^{-1}$, and $G^<{}_0(k,\omega)=-2\,\mathrm{Im}[G^+{}_0(k,\omega)]f(\omega-\mu)$.

(ii) In order to take advantage of the local character of the electron-hole interaction, we use the Fourier transform of the Green's functions of Eq. (1), $G(1,2)$, which actually have only a spatial dependence on $r=x_1-x_2$ as the system is homogeneous. We calculate the free pair propagator defined as

$$H(1;2)=iG(1,2)G(1,2). \tag{10}$$

The retarded and correlation parts are calculated passing from the Keldysh contours to the usual time axis:

$$H^<(r,t)=iG^<(r,t)G^<(r,t), \tag{11}$$

$$H^+(r,t)=iG^+(r,t)G^+(r,t)+2iG^+(r,t)G^<(r,t). \tag{12}$$

The dependence on the relative distance has been explicitly shown. The dependence on the relative propagation time $t=t_2-t_1$ stems from the stationary condition. The pair propagator is then Fourier transformed to (k,ω) space.

(iii a) For the Born approximations, we use Eq. (7):

$$T^+(q,\omega)=-1+H^+(q,\omega), \tag{13a}$$

$$T^<(q,\omega)=H^<(q,\omega). \tag{13b}$$

(iii b) For the SCLA case, Eq. (9) is readily solved as

$$T^+(q,\omega)=-[1+H^+(q,\omega)]^{-1}, \tag{14a}$$

$$T^<(q,\omega)=|T^+(q,\omega)|^2H^<(q,\omega). \tag{14b}$$

(iv) The electron self-energy is then calculated in real space as in Eq. (6). The retarded and correlation functions, defined on the usual time axis, read

$$\Sigma^<(r,t)=iT^<(r,t)G^>(-r,-t)=-iT^<(r,t)[G^>(r,t)]^*,$$

$$\Sigma^+(r,t)=+iT^<(r,t)G^-(-r,-t)+iT^+(r,t)G^<(-r,-t)$$
$$=+iT^<(r,t)[G^+(r,t)]^*-iT^+(r,t)[G^<(r,t)]^*.$$

(v) The new electron Green's functions are then calculated as

$$G^+(k,\omega)=[\omega-k^2/4-\Sigma^+(k,\omega)+i\gamma]^{-1},$$
$$G^<(k,\omega)=-2\,\mathrm{Im}[G^+(k,\omega)]f(\omega-\mu). \tag{15}$$

The procedure is repeated through step (ii) until self-consistency is reached. Fast Fourier transforms are performed on a finite grid of 16384×128 points for the frequency and wave-vector domains, respectively. The frequency and wave-vector domain (k,ω) is $(-20,20)\times(-3,3)$. Due to the finite k range, we obtain $E_b=0.4$. The external $\gamma>0$ in step (v) is adiabatically switched off during self-consistency. In this way the imaginary part of the final G is provided by the interaction only. For the non-self-consistent Born approximation (or Markov-Born), we use the frequency-independent, on-pole $\Sigma^+_k(\omega=k^2/4)$ in the Green function, and stop the procedure at step (v).

All of the considered approximations are conserving in the sense of Baym and Kadanoff:[18] the total density, total momentum, total energy, and total angular momentum of the system are conserved. This is a fundamental property of any approximation for the self-energy; otherwise unphysical results may result. We will come back to this point again in the calculation of the optical response of the system in the various approximations.

The polarized electron-hole gas with a contact potential interaction that we consider here can be mapped onto a single-band Hubbard model with spin 1/2 and attractive interaction, in the limit of infinite width of the band, and infinite on-site interaction so as to produce finite E_b (continuum limit). For the Hubbard model with a repulsive interaction, the self-consistent ladder approximation is known as the fluctuation exchange approximation (FLEX).[19] Even though in this repulsive case the opening of a Hubbard gap is not reproduced, in the attractive case the gap is of a different nature and is notoriously well described within this approximation.[20]

III. SINGLE-PARTICLE PROPERTIES

We plot in Fig. 2 the electron spectral function at $k=0$ for different densities obtained in the SCLA. The temperature $T=0.1\ll E_b=0.5$. For this particular figure we used the k range $(-6,6)$ in the numerical solution. For $n\sim0.001$ the electron spectral function has a very narrow Lorentzian shape. For larger densities, a satellite structure appears in the low-energy side of the spectral function. This structure is located at the exciton binding energy, below the main peak,

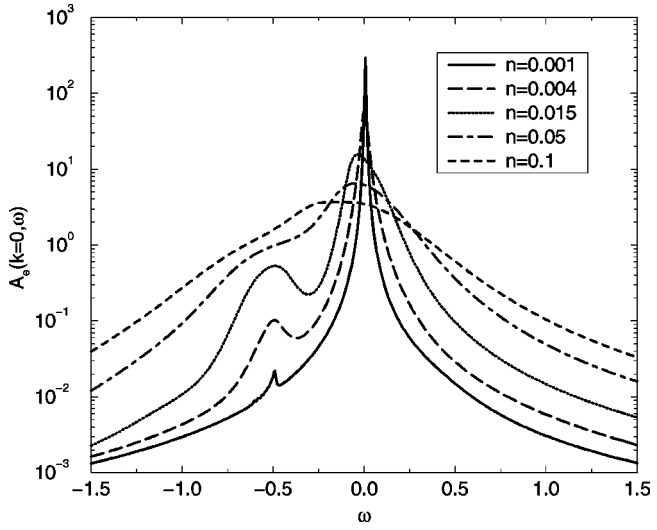

FIG. 2. Electron spectral function at $k=0$ as a function of the total carrier density. $T=0.1$.

and accounts for the correlation of the electron at $k_e=0$ bound with holes in other k_h states. Excitons with all values of the center of mass wave vectors are involved in this peak,[8] as we will also show in the next section. This correlation structure is of course not present in the Born approximations, which maintain their single quasiparticle peak structure at any density. As the density rises, the relative weight of the satellite structure in the SCLA spectral function with respect to the main quasiparticle peak increases. Moreover, both structures become broader. For densities $n>0.1$, it becomes difficult to distinguish between the excitonic and the main peak, and a single, broad, redshifted quasiparticle structure appears.

In Fig. 3 we show the imaginary part of the electron self-energy for different densities. We will also refer in the following to this quantity as (energy-dependent) broadening. In the SCLA $\mathrm{Im}(\Sigma)$ shows two peaks corresponding to dephasing experienced by an unbound or a bound state propagated in the system. Both peaks increase with density. At low density, $n=0.01$, dephasing at the exciton energy dominates, while at $n=0.05$ both peaks become comparable. In the SCBA, the peak of $\mathrm{Im}(\Sigma)$ at $-E_b$ is obviously absent, as propagation of bound pairs is not allowed in the theory. Instead at low density $n=0.01$, the broadening at the main quasiparticle energy ($\omega=0$) is similar in the SCLA and SCBA. Indeed, few excitons are expected in the plasma, and scattering mainly originates from free carriers. A heuristic understanding may be obtained with the action mass law relating the concentration of different chemical species in a reaction. In our case, electron+hole $\leftrightarrow$ exciton, and the law states $n_c^2/n_X=n^*(T)$, where n_c and n_X represent the density of unbound carriers and excitons, respectively. $n^*(T)$ is a crossover density that depends only on the temperature, and at $T=0.1$, $n^*\sim 0.005$. For $n<n^*$, $n_X\ll n$. Therefore, a small density of excitons is expected at $n=0.01\sim n^*$. At this density the exciton–free-carrier contribution to free-carrier broadening is weaker than the free-carrier–free-carrier contribution. At larger density, bound excitons in the plasma

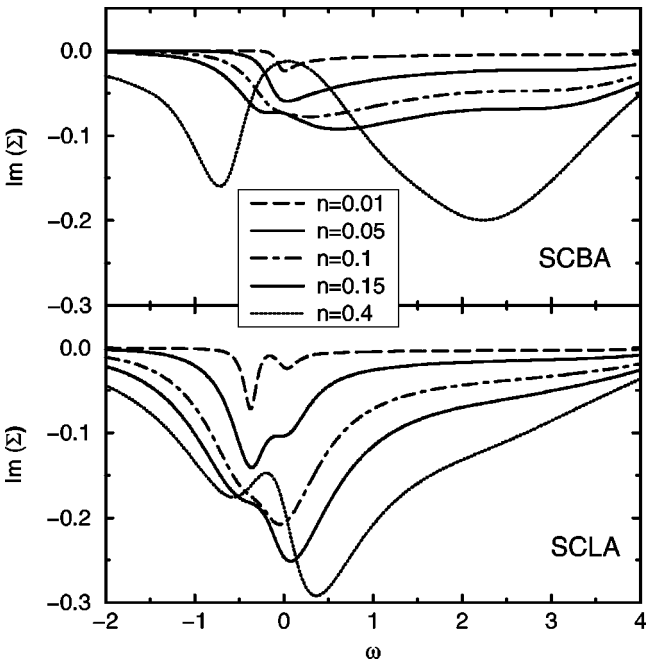

FIG. 3. Self-energy $\Sigma(k=0,\omega)$ for $T=0.1$ and different densities given in the figure, in the self-consistent Born approximation (SCBA) and self-consistent ladder approximation (SCLA).

become dominant, and broadening at the quasiparticle peak becomes much larger in the SCLA than in SCBA. This trend is observed up to $n=0.15$, indicating the relevance of correlated states in the plasma even at this large density. However, the heuristic interpretation of the broadening based on the action mass law given above becomes meaningless, as it is not possible to distinguish between two chemical species anymore. At the highest considered density $n=0.4$, we clearly observe a dip to very small broadening in the self-energy for the SCBA case. This dip is around the Fermi energy and accounts for the blocking of the scattering inside the Fermi sea. In fact, only at this large density does the Fermi gas become degenerate (Fermi energy much larger than T). In the SCLA, the broadening never vanishes but is only partially reduced at the Fermi level. This is indicative of a more complicated structure of the electron-hole plasma and of the broadening process, where Pauli blocking looses much of its effectiveness, and is suggestive of a non-Fermi liquid behavior. We finally noticed that $\mathrm{Re}(\Sigma)$ is comparable to $\mathrm{Im}(\Sigma)$ at any density in the SCLA, and thus felt that the excitonic satellite peak in the spectral function does not correspond to a zero of $\omega-\mathrm{Re}[\Sigma(\omega)]$. Indeed, we do not expect the appearance of another simple quasiparticle in the plasma. For $\omega\sim -E_b$, and for $E_b\gg|\mathrm{Im}(\Sigma)|$, we have $A_{k=0}\sim|\mathrm{Im}(\Sigma)|/|E_b|^2$. Thus, the correlation satellite in the spectral function follows the peak of $\mathrm{Im}(\Sigma)$ at $\omega=-E_b$.

In Fig. 4 we show the density dependence of the electron (or hole) chemical potential as a function of the density for $T=0.1$, in the three considered approximations. At very low density, $n\ll 0.01$, the chemical potential is $\mu\ll -0.4$, and its value is similar in all approximations. In this case, we are describing free electron-hole pairs, as also suggested by a law of mass action, which gives a crossover density of about

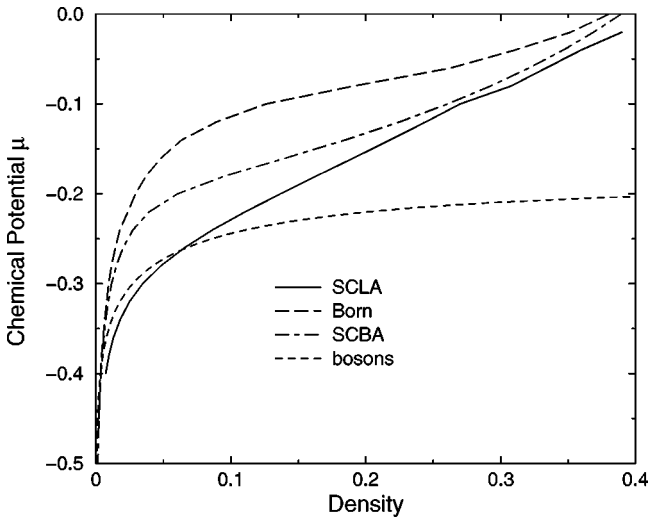

FIG. 4. Chemical potential μ in the three approximations, at $T=0.1$. The short-dashed line shows half the chemical potential of noninteracting bosons, with ground state energy of $-E_b$.

$n^*=0.005$ at $T=0.1$. In this case the description of μ is rather good even in approximations that neglect the existence of bound states.

However, for $n>0.01$, the chemical potential in the Born approximations is much larger than for the SCLA. In fact, in the SCLA we are also describing the fraction of cold interacting excitons in the plasma. As the ground state energy of this part of the plasma is at about $-E_b$, the total energy of the system is thus reduced with respect to that of a gas of unbound particles. In order to clarify this point further, we plot on the same graph half of the chemical potential of bosons at a ground state energy of $-E_b$ and mass equal to the exciton mass. This is the chemical potential of a gas of electron (and holes) completely bound into bosonic excitons. The halving comes from the equilibrium condition $\mu_X=\mu_e+\mu_h=2\mu$. The chemical potential of bosons compares reasonably well with the chemical potential calculated in the SCLA, up to $\mu<-0.25$, $n<0.1$. Above this limit, the chemical potential from the SCLA grows faster. There are two reasons for this faster growth: first, the exciton gas is repulsively interacting, second, the exciton gas eventually ionizes into free carriers. At densities $n>0.2$, the SCLA and SCBA are indeed comparable, and at even larger density, the MBA is also reasonable. This shows that the SCLA is a powerful tool for the investigation of the intermediate regime of densities, where deviations from both the (noninteracting) bosonic and pure fermionic models are important.

IV. MAPPING THE SCLA TO A BOSONIC MODEL AT LOW DENSITY AND TEMPERATURE

In Fig. 5 we plot $A(k,\omega)$ for $T=0.043$ and $n=0.02$. We can observe the parabolic dispersion of the main quasiparticle peak, broadened by the scattering (white region in the plot). Broadening is larger at small k due to the larger phase space in one dimension. For $\omega<0$, we have the correlation structure shown for $k=0$ in Fig. 2, which is also present at larger k. We remark that this region of correlated electrons

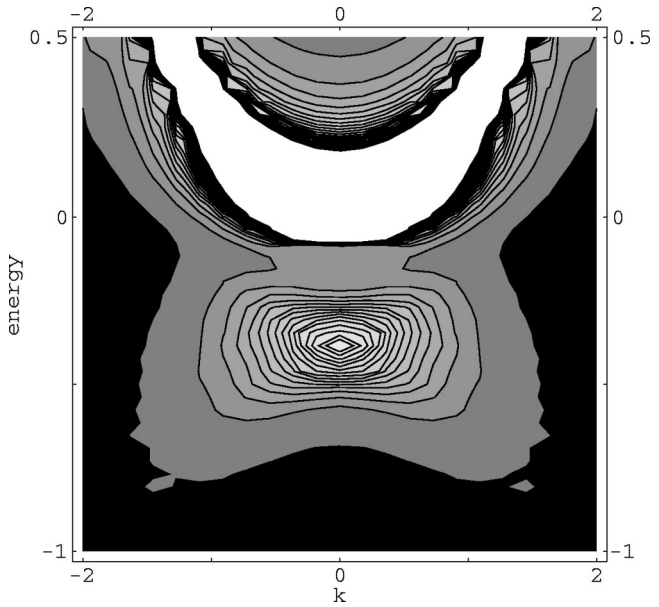

FIG. 5. Contour plot of $A_e(k,\omega)$ at $T=0.04$ and $n=0.02$.

extends into a region of k of the order of 1 (i.e., of a_B^{-1}). Its shape (dispersion) is related to the exciton wave function, as we show in the following.

In a low-density, low-temperature limit, we can start to consider $G=G_0$, and analytically calculate the retarded pair propagator $H^+(k,\omega)$ from Eq. (12), neglecting $G_0^<$, which is of the order of the density. We obtain

$$H^{(0)+}(k,\omega)\sim\frac{-1}{\sqrt{2}\sqrt{\omega-k^2/8+2i\gamma}},$$

where $\gamma>0$ is the usual regularization number. Solving for the T matrix with the Bethe-Salpeter equation (14a) and expanding around its pole, we obtain

$$T^{(0)+}(k,\omega)=\frac{1}{\omega+\frac{1}{2}-k^2/8+2i\gamma}.$$

Thus, the T matrix at the lowest order for the contact potential has the form of a free propagator, for particles at an energy $-1/2+k^2/8$, having a mass that is twice the electron mass, i.e., the electron plus hole mass. Expanding the Bethe-Salpeter equation to higher order, we obtain

$$T^{(1)+}(k,\omega)=T^{(0)+}(k,\omega)H^{(1)+}(k,\omega)T^{(0)+}(k,\omega).$$

Therefore, we may interpret $T^{(0)+}(k,\omega)$ as the free-exciton (boson) Green function, and $H^{(1)+}(k,\omega)$ as the lowest-order self-energy.[21] In particular,

$$H^{(1)}(1,2)=2iG^{(1)}(1,2)G_0(1,2), \tag{16}$$

$$\begin{aligned} G^{(1)}(k,\omega)&=G_0(k,\omega)\Sigma^{(0)}(k,\omega)G_0(k,\omega),\\ \Sigma^{(0)}(1,2)&=iT^{(0)}(1,2)G_0(2,1). \end{aligned} \tag{17}$$

As $T^{(0)}(k,\omega)$ is peaked close to $\omega=-1/2$, we may neglect $G_0^<(k,\omega)$ in this region, and use

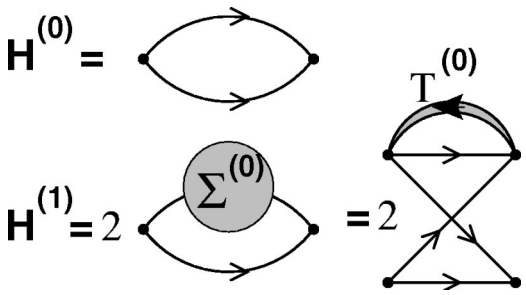

FIG. 6. The perturbation expansion to lowest order for the boson (exciton) self-energy, and the four-particle vertex $F^{(0)}$. Thin lines are the bare electron (or hole) propagator. The shaded two-particle Green function is the bare exciton propagator.

$$\Sigma^{(0)+}(k,\omega)\sim i\int \frac{dq\,d\omega'}{(2\pi)^2}T^{(0)<}(q,\omega')G_0^-(k+q,\omega+\omega').$$

Integrating around $\omega'=-1/2$, we obtain

$$\Sigma_k^{(0)+}(\omega)\sim\frac{n}{\omega+\frac{1}{2}+k^2/8+i\gamma},$$

where n is the total density. This is the structure shown in Fig. 3 at $\omega=-1/2$, which produces the satellite correlation peak in the electron spectral function, shown in Fig. 5. We also notice that this structure has *negative* dispersion, as is also apparent in Fig. 5.

We can now define an exciton-exciton interaction at low density, from Eqs. (16) and (17) above, which are pictorially shown in Fig. 6. We thus define a four-point interaction kernel $F^{(0)}$, and the boson self-energy $H^{(1)}(1,2)$ is written as

$$H^{(1)}(1,2)=\int d\bar{1}d\bar{2}F^{(0)}(1,2;\bar{1},\bar{2})T^{(0)}(\bar{2},\bar{1}). \qquad (18)$$

We can see from Fig. 6 that $F^{(0)}$ represents the electron (or hole) exchange in the scattering of the two excitons. Thus

$$F^{(0)}(1,2;1'2')=2iG_0(1,2)G_0(1',2')G_0(1,2')G_0(1',2). \qquad (19)$$

If we neglect retardation (or memory) effects, we may define an instantaneous potential at the exciton energy using $\tau_1=\tau_2$, $\tau_{1'}=\tau_{2'}$ and calculating the resulting F at the exciton frequency $\omega_0=-1/2=E_B$. For simplicity, we also use $k,k'\sim 0$ for the incoming excitons, and find

$$\begin{aligned}F^{(0)}(q,\omega_0)\sim 2i\sum_{q',\omega'} & G_0^+\left(q',\frac{\omega_0}{2}+\omega'\right)\\ &\times G_0^+\left(-q',\frac{\omega_0}{2}-\omega'\right)\\ &\times G_0^+\left(q-q',\frac{\omega_0}{2}+\omega'\right)G_0^+\left(q'-q,\frac{\omega_0}{2}-\omega'\right)\\ &=\frac{64}{q^2}\frac{2\sqrt{4+q^2}-(4-q^2)}{(4+q^2)^2}. \qquad (20)\end{aligned}$$

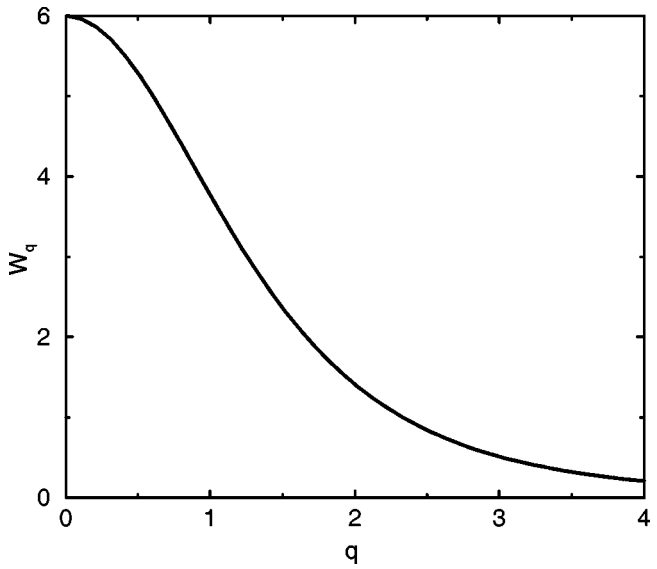

FIG. 7. The exciton-exciton interaction potential $W_q=F^{(0)}(q,\omega_0)$.

This function rapidly drops to zero at $q>1$ as expected, and $F^{(0)}(0,\omega_0)=6$. This value is also obtained from standard boson-boson exchange-interaction expressions (see, e.g., Ref. 22) when only the electron-hole interaction is used. We show the full structure of $F^{(0)}(q,\omega_0)$ in Fig. 7.

We are now in a position to discuss some of the qualitative changes introduced by simplifying the Coulomb interaction to an on-site one. In the limit of low density, we may in fact compare the exciton-exciton interaction calculated above with that calculated using a realistic Coulomb interaction, as a standard boson-boson exchange expression at small momenta exists.[23] In a realistic wire, a short-range cutoff is introduced by the finite size of the electron and hole wave functions in the confinement directions. A typical cutoff is of the order of the Bohr radius or smaller. Typically, we have to consider tight confinements in order to avoid participation of higher confined levels into the exciton wave function. The Coulomb interaction is then reasonably represented by a function $V_r=A/(r+r_0)$, where r_0 is a cutoff distance, and A is then chosen such that $E_b=-1/2$. We used $r_0=0.1$, and $A=0.18$. In this case the resulting Bohr radius is 1, indicating tight confinement of the carriers in the confinement plane. The exciton-exciton exchange interaction at small q is calculated in the small $q\ll a_B^{-1}$ limit,

$$\begin{aligned}W_{xx}=2\sum_{k,k'} & V_r(k-k')\phi_{1s}(k)\phi_{1s}(k')\\ &\times[|\phi_{1s}(k)|^2-\phi_{1s}(k)\phi_{1s}(k')]\sim 1.4, \qquad (21)\end{aligned}$$

where $\phi_{1s}(k')$ is the $1s$ wave function of the exciton. The positive term in Eq. (21) is the exchange term due to the attractive electron-hole interaction, while the negative term is due to the electron-electron and hole-hole repulsive interactions. In the δ-function-like potential the negative term is absent because of locality. In the long-range case instead, the electron-electron and hole-hole interactions largely cancel

the electron-hole interaction in the exchange integral, resulting in an exciton-exciton interaction that is four times smaller when compared with the value of 6 obtained for $F^{(0)}(q=0,\omega_0)$. We conclude that local interaction leads to an overestimation of the boson-boson interaction at a given density and therefore of broadening. However, this does not imply that broadening effects are *qualitatively* different. Moreover, we also stress that this overestimation does not concern at all the comparison of the SCLA with the other simpler approximations considered in this work, as all are carried out using the same interaction potential.

V. OPTICAL PROPERTIES

We now consider interaction of the electron-hole system with a transverse electromagnetic field in the dipole approximation:

$$H_P=\sum_{\mathbf{q},q} C_{\mathbf{q},q}(a_{\mathbf{q},q}P_q^\dagger+a_{\mathbf{q},q}^\dagger P_q), \tag{22}$$

where

$$C_{\mathbf{q},q}=\frac{ep_{cv}}{m_0c}\sqrt{\frac{4\pi\hbar c}{q_tV}}I_\parallel(\mathbf{q}),$$

is the dipole matrix element, which includes also the overlap integral of the electromagnetic field with the confined carriers $I_\parallel$. Here $\mathbf{q}$ represents two-dimensional (2D) wavevectors in the plane orthogonal to the wire axis, q are wave vectors along the wire, while $q_t^2=\mathbf{q}^2+q^2$, m_0 is the free-electron mass, c the velocity of light, and p_{cv} the momentum matrix element between the conduction and hole bands. $a_{\mathbf{q},q}$ is the photon destruction operator, and P_q is the polarization operator, defined as $P_q=\Sigma_k d_{q-k}c_k$, i.e., local in real space in the dipole approximation. As the section of the wires is always much smaller than the wavelength of light, we have $I_\parallel\sim 1$. Moreover $q_t\sim E_{\mathrm{gap}}/(\hbar c)$ is almost constant; thus we use arbitrary units from now on, with $C=1$. Actual values of absorption and gain are easily calculated by using the appropriate value of C for the given material.

In the process of scattering of light from the system, an absorbed photon creates a coherent electron-hole pair that propagates in the crystal, interacts with the background plasma, then recombines, and a photon is emitted. When we introduce photon propagators, the interaction process is represented by a photon self-energy. We will not solve the photon Dyson equation, nor we will dress the electron and hole propagation with the photon interaction. In other words, we neglect both polaritonic effects and higher-order nonlinear interactions. In fact, we are restricting our attention to weak external fields, i.e., assuming interaction of the plasma with the photon field to be weak. Otherwise, it could be possible for the system to be driven out of equilibrium, because the photon chemical potential is zero and far below that of the electron-hole plasma. This equilibrium condition is well fulfilled in real systems, and an exception made for the strongest laser fields. Within this weak-interaction approximation, the photon self-energy is exactly given by the pair correlation function

$$\Pi_q(\tau,\tau')=\langle TP_q^\dagger(\tau)P_q(\tau')\rangle. \tag{23}$$

However, this correlation function has to be calculated within some approximation, and also using approximate propagators. The resulting self-energy may not be conserving. In particular, particle flux conservation at the vertex translates in the longitudinal *f*-sum rule,[18] which has to be respected in any reasonable approximation.

In order to shed light on this important issue, we consider the problem of interaction of photons with the plasma from a different viewpoint. As we are only interested in the linear response to the external electromagnetic field, the correct photon self-energy is also given by the linear response of the plasma to a *classical* electromagnetic field, i.e., considering the photon creation and destruction operators in Eq. (22) as c numbers. Baym and Kadanoff give a method for constructing a conserving expression for this response function in Ref. 18. When an external coherent electromagnetic field is applied to the plasma, coherence develops in the plasma, and pair propagators additionally have to be defined along with the single-particle propagators. They are analogous to anomalous propagators in the theory of superconductivity. The electron-hole anomalous propagator reads

$$G_{eh}(1,2)=i\langle Td(2)c(1)\rangle. \tag{24}$$

Times are defined on the Keldysh contour as usual. Another anomalous propagator G_{he} can be similarly defined for convenience, and notation regrouped into a matrix notation, as for Nambu propagators in the problem of superconductivity.[24] The Dyson equation (5) is extended to include both anomalous propagators and the external interaction H_p:

$$\begin{aligned}\int d\bar{2}G_0^{-1}(1,\bar{2})G(\bar{2},3)&=\delta(1,3)+\int d\bar{4}\Sigma(1,\bar{4})G(\bar{4},3)+\int d\bar{4}\Sigma_{eh}(1,\bar{4})\\&\quad\times G_{he}(\bar{4},3)-A(1)G_{he}(1,3)\end{aligned} \tag{25}$$

,

$$\begin{aligned}\int d\bar{2}G_0^{-1}(1,\bar{2})G_{eh}(\bar{2},3)&=\int d\bar{4}\Sigma(1,\bar{4})G_{eh}(\bar{4},3)+\int d\bar{4}\Sigma_{eh}(1,\bar{4})G(\bar{4},3)\\&\quad-A(1)G(3,1).\end{aligned} \tag{26}$$

As a general rule for generating a conserving approximation, the self-energies have to be obtained from the functional derivation of a grand potential with respect to the propagators. The normal self-energies have been already introduced. For the anomalous self-energy $\Sigma_{eh}(1,2)$, we need to generalize the expression of the grand potential including terms where the normal propagators are replaced by the anomalous ones. The anomalous propagators G_{eh} are at least first order in the external potential A, as spontaneous symmetry breaking is ruled out by the Mermin-Wagner theorem.

For the linear response, we need the anomalous self-energy Σ_{eh} up to linear terms in the external potential only, thus at most linear terms in the anomalous propagators. Consequently, we need at most quadratic terms in these propagators in the grand potential to obtain the Σ_{eh} from the functional derivative. We conclude that the only term to be considered is the anomalous Fock term, which is the usual Fock term with anomalous propagators replacing normal ones. As the approximation is conserving, we are also guaranteed that absorption fulfills the *f*-sum rule[18] for any value of density and temperature. The anomalous self-energy obtained from the anomalous Fock term reads

$$\Sigma_{eh}(1,2) = -iG_{eh}(1,2) + O(A^2). \tag{27}$$

Normal G are at least second order in the external potential A, while both G_{eh} and Σ_{eh} are at least first order. The anomalous Dyson equation (26) to lowest order becomes

$$\int d\bar{2} G^{-1}(1,\bar{2}) G_{eh}(\bar{2},3) = -i \int d\bar{4} G_{eh}(1,\bar{4}) G(\bar{4},3) - A(1)G(1,3). \tag{28}$$

Introducing the response function

$$\tilde{\Pi}(1,2) = -i \left. \frac{\delta G_{eh}(1,1)}{A(2)} \right|_{A=0}, \tag{29}$$

and taking the first-order variation of Eq. (28), we obtain the equation for $\tilde{\Pi}(1,2)$:

$$\tilde{\Pi}(1,2) = iG(1,2)G(1,2) - i \int d\bar{3} G(1,\bar{3}) \times G(1,\bar{3}) \tilde{\Pi}(\bar{3},2) H(1;2) - \int d\bar{3} H(1;\bar{3}) \tilde{\Pi}(\bar{3},2), \tag{30}$$

which is easily solved and gives

$$\tilde{\Pi}(1,2) = H(1;2) + \int d\bar{3} d\bar{4} H(1;\bar{3}) T(\bar{3};\bar{4}) H(\bar{4};2). \tag{31}$$

It is straightforward to show that $\tilde{\Pi}(1,2)$ obeys bosonic Kubo-Martin-Schwinger relations, as both H and T do. In particular, we have

$$\tilde{\Pi}^{+}(q,\omega) = H^{+}(q,\omega) |T^{+}(q,\omega)|^2, \tag{32}$$

$$\tilde{\Pi}^{<}(q,\omega) = H^{<}(q,\omega) |T^{+}(q,\omega)|^2. \tag{33}$$

Absorption $\alpha(\omega)$ and photoluminescence $\mathrm{PL}(\omega)$ at $q=0$ are derived as $\alpha(\omega) = -\mathrm{Im}[\Pi^{+}(0,\omega)]$ and $\mathrm{PL}(\omega) = -\mathrm{Im}[\Pi^{<}(0,\omega)]$, respectively.

We remark that terms of order higher than the anomalous Fock term have to be considered in the anomalous self-energy expansion when a *finite* external field is present, such as in the case of a strong laser field. Anomalous Born terms calculated in the Markov approximation have been considered in the semiconductor Bloch equations by Lindberg and Koch in Ref. 25, and called polarization-polarization scattering terms. Here we do not further pursue such extensions, which are clearly beyond the scope of the present paper. We only note that our approach is easily extended to such conditions, while keeping full control of the conservation laws.

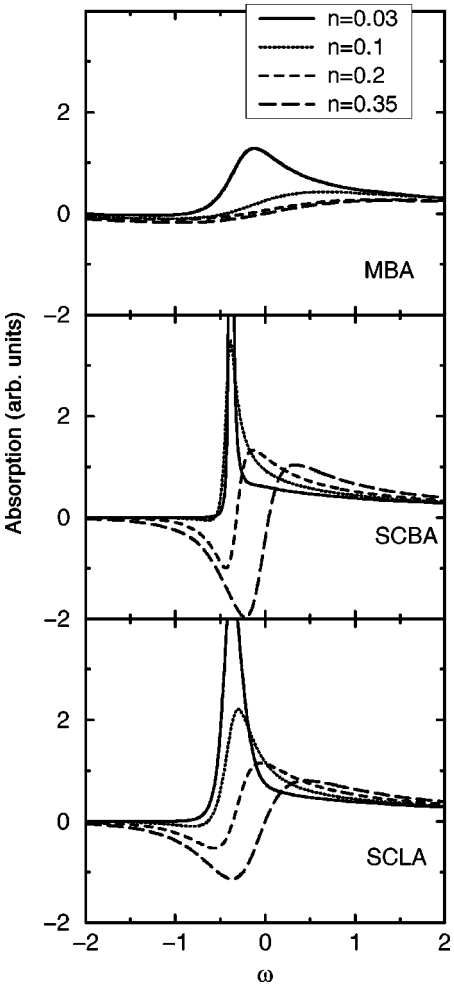

FIG. 8. Absorption spectra in the Markof-Born approximation (MBA), self-consistent Born approximation (SCBA), and self-consistent ladder approximation (SCLA) for different densities indicated in the figure.

A. Optical spectra and stability of the excitonic emission

We show in Fig. 8, the absorption spectra in the normal direction ($q=0$) at $T=0.2$, for different densities, in the MBA, SCBA, and SCLA. In the absorption spectrum, we note the characteristic excitonic peak and the continuum absorption at low density. The exciton linewidth is extremely narrow in the SCBA, and much broader in the MBA. The SCLA linewidth is intermediate. In the SCBA there is a very small broadening at the exciton energy, as no excitons are represented in the theory, while in the MBA, the free-carrier broadening at $\omega=0$ is assumed. This is somewhat larger than the broadening in the SCLA at $T=0.2$. For large den-

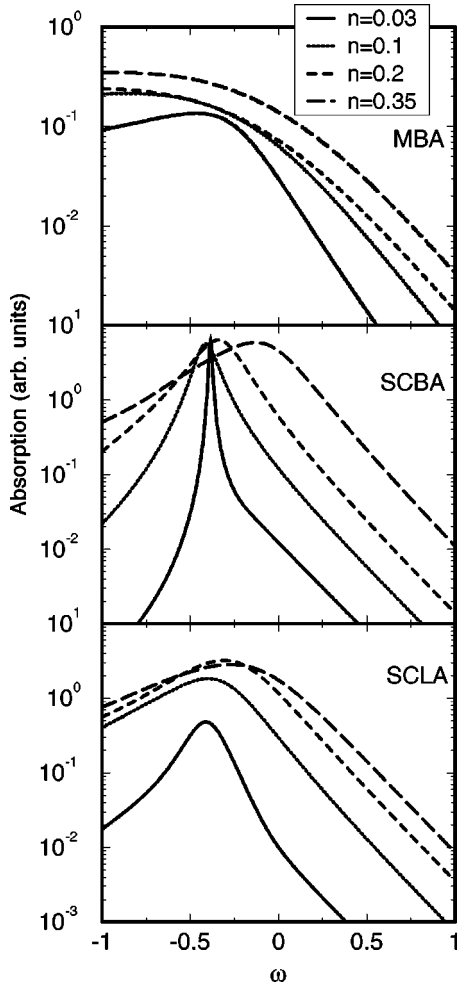

FIG. 9. Photoluminescence spectra in the MBA, SCBA, and SCLA for different densities indicated in the figure.

sities $n>0.2$, the excitonic peak is bleached in all approximations, and a region of negative absorption, i.e., optical gain, appears. The absorption changes sign at $\omega=\mu_e+\mu_h=2\mu$, coinciding with the change of sign of the Bose factor and resulting in a well defined—i.e., positive—photoluminescence through the Kubo-Martin-Schwinger relation.

We plot the emission or PL spectra in Fig. 9. First we notice the different scale for the MBA, where a smaller peak emission is calculated even for the largest considered densities. For large density $n>0.2$, we observe a saturation of the intensity. This can be understood in terms of the fermionic nature of the carriers, when the electron-hole plasma becomes degenerate. Second, we notice excitonlike emission even when excitonic absorption is bleached in all models. In fact, vertex corrections place the free-carrier emission at the exciton energy, even when no bound excitons are described in the gas.

Eventually, only at very small density do the free-carrier and excitonic emission become distinguishable, as we notice an exponential emission shoulder at high energy $\omega>0$ in the SCLA and SCBA, reminding us of a fermionic emission tail at small degeneracy (Boltzmann distribution). At larger density, the two features at different energy merge into a unique one, due to increased broadening. A single peak is also observed in experiments, where finite noise in the data and large inhomogeneous broadening mask any minor feature.[17] For this reason, it is in practice very delicate to establish the position of the band gap (bottom of the free-carrier bands) directly from emission data.[26] Third, we note that the low-energy shoulder of the PL emission in the MBA is Lorentzian because of the Markov approximation, and the broadening is largely overestimated also at low energies. The linewidth in the SCBA is instead underestimated at low density, as for absorption.

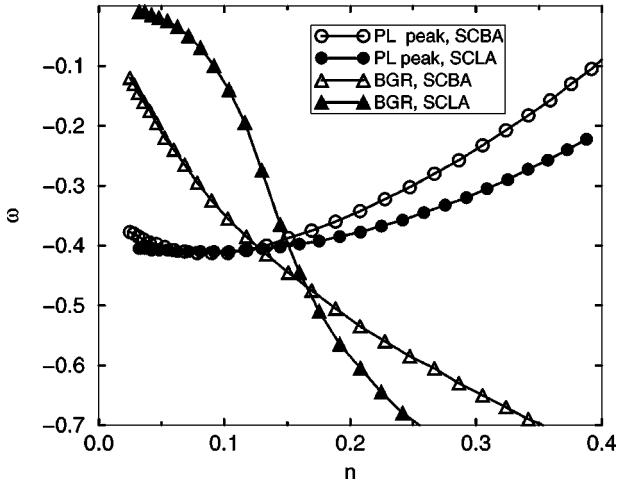

FIG. 10. The band-gap renormalization (BGR) and emission peak energy in the SCBA and SCLA as indicated in the figure.

An interesting—and directly observed—physical quantity is the energy of the PL peak. As noted above, emission is excitonic due to the correlation of the coherent electron-hole pair emitted. In Fig. 10 we plot the position of this peak in the PL as a function of the carrier density, together with the band-gap renormalization (BGR) defined as twice the energy of the main peak of the spectral function. Interestingly, exciton bleaching in absorption appears at a density that is comparable to the density where the band-gap renormalization crosses the emission energy, i.e., $n\sim0.15$. There are two interesting features to be observed in Fig. 10: first, the band-gap renormalization is negligible in the SCLA for $n<0.1$; second, emission energy is constant in this range of densities and blueshifting less than that in the SCBA for larger density. Comparison with the MBA is vitiated by excessive broadening in this approximation. The simple Hartree-Fock approximation instead gives results that are similar to those obtained in the SCBA for the band-gap renormalization and the PL emission peak, apart from more pronounced blueshifts.[10] Stability of the emission peak is usually interpreted as a partial compensation of the self-energy and vertex corrections. Since in the Hartree-Fock approximation the broadening effects are missing, we deduce that these effects are indeed relevant for the cancellation found in the SCBA and in the SCLA at high density and explain the reduction of the blueshift with respect to simple Hartree-Fock calculations.

B. Excitonic gain

Optical gain is usually considered in the regime of degenerate electron-hole plasma. In this regime, spectral functions can be assumed to be simple Lorentzians, and the absorption can be written as

$$\alpha(\omega) \propto \int \frac{dk}{2\pi} \frac{1-2f(k^2/4-\mu)}{(\omega-k^2/2)^2+\gamma^2}, \tag{34}$$

where γ is the spectral broadening. Then, negative absorption or gain occurs only when the Pauli blocking factor $[1-2f(k^2/4-\mu)]$ becomes negative, which necessarily requires a chemical potential above the band gap, or in other words, inversion. However, both vertex corrections and deviations of the spectral function from simple Lorentzian should be taken into account at lower density and temperature. In this case, the absorption can be written as

$$\alpha(\omega) \propto |T^+(q=0,\omega)|^2 \int \frac{dk}{2\pi} \frac{d\omega'}{2\pi} [1-f(\omega-\omega'-\mu) - f(\omega'-\mu)] A_k(\omega-\omega') A_k(\omega'), \tag{35}$$

The term in square brackets $1-f(\omega-\omega'-\mu)-f(\omega'-\mu)$ is the generalization of the Pauli blocking factor for a system where the quasiparticles are described by arbitrary spectral functions, and clearly one of the Fermi functions refers to electron occupation, the other to hole occupation. This expression of the absorption is valid only in the case of the short-range potential, and for the long-range case T^+ depends also on the relative momentum of the pair k and becomes part of the integral kernel. Using the definition of Fermi and Bose functions, the absorption can be recast in the form

$$\alpha(\omega) = \frac{|T^+(q=0,\omega)|^2}{g(\omega-2\mu)} \int \frac{dk}{2\pi} \frac{d\omega'}{2\pi} f(\omega-\omega'-\mu) \times f(\omega'-\mu) A_k(\omega-\omega') A_k(\omega'), \tag{36}$$

where $g(\omega-2\mu)$ is the Bose function. Therefore, gain clearly occurs below twice the chemical potential μ (i.e., $\mu_e+\mu_h$), even when the chemical potential is *below* the band gap. However, for it to be sizable, the spectral functions must have non-negligible weight in this region of the spectrum. In the MBA and SCBA cases, this weight is clearly given by broadening effects alone, while in the SCLA it is also due to the presence of the excitonic correlation peak in the spectral function as shown in Fig. 2. A sizable enhancement of the gain is found in correspondence to the excitonic resonance because of the vertex correction, given by the $|T^+|^2$ factor in Eq. (36). When $2\mu<-E_B$, both gain and excitonic absorption coexist. In this case, we talk of *excitonic gain*. The system is inversionless in the sense of Eq. (34) above. However, only in the SCLA do we describe gain due to the presence and scattering of excitons in the low-temperature, low-density plasma, while in the other approximations, gain is purely related to dynamical effects in the interaction vertex with the photon.

In Fig. 11 we plot the absorption spectra close to the exciton resonance at $T=0.1 \ll E_B$. For the considered densities $n<0.1$, gain coexists with the excitonic resonance in absorption. Only for the MBA at $n=0.1$ is the absorption peak completely shifted to higher energies, and we can no longer speak of excitonic absorption. As usual, the broadening in the exciton spectral region is too small and unphysical in the SCBA, resulting in very sharp and unphysical features. Gain in the SCLA is instead over a larger spectral region, and its value is larger than that predicted in the MBA at large density $n>0.3$ shown in Fig. 8. Excitonic gain clearly originates from inclusion of excitons in the plasma for the SCLA. In fact, reasonable broadening is calculated in the exciton spectral region, mainly originating from exciton-exciton scattering as shown in Sec. IV. We conclude that the SCLA indicates that sizable excitonic gain can be obtained at moderate density and temperature, in a reasonably large spectral region of the order of a fraction of E_B.

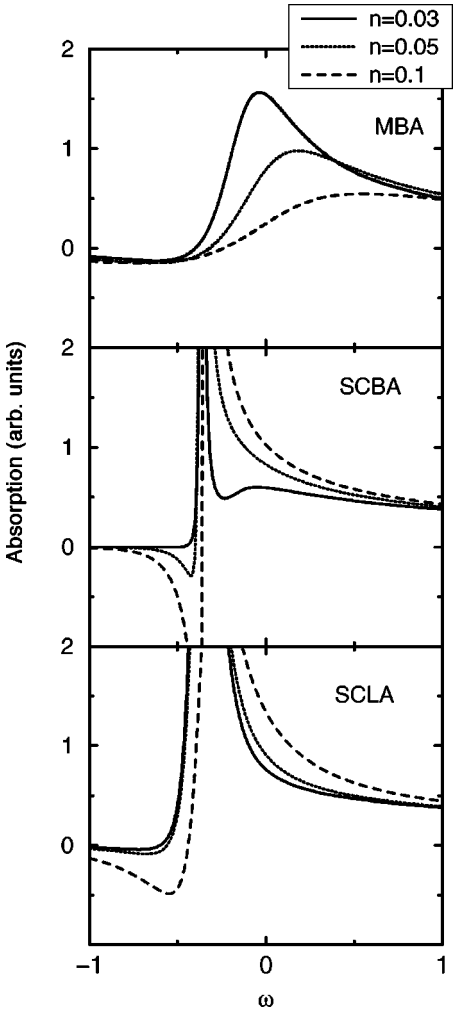

FIG. 11. Absorption spectra at $T=0.1$ for the MBA, SCBA, and SCLA, and low densities indicated in the figure.

Excitonic gain has been widely studied in II-VI quantum wells.[27] However, these are two-dimensional systems, and excitonic correlations are expected to be less pronounced in this systems, so at this stage it is not reasonable to make even a qualitative comparison. For quantum wires, sizable gain at 10 K ($T\sim0.05$) for an estimated carrier density well below

the Mott transition has been recently claimed by Sirigu *et al.*[28] This is a first indication that excitonic gain might be relevant in these systems. However, a qualitative and quantitative understanding of this experiment is clearly premature. From the experimental side, inhomogeneous broadening due to interface disorder has to be decreased well below the binding energy, while a more realistic Coulomb interaction has to be addressed by the theory.

VI. CONCLUSIONS

We have presented a model that includes excitonic correlation in the description of a highly excited semiconductor quantum wire. The model has been simplified using a short-range potential and consideration of a polarized gas. Correlation has been calculated self-consistently at the ladder level (SCLA). We have shown that bound states appear as a low-energy correlation peak in the spectral function of electrons and holes. We compared the results obtained with the SCLA to the ones obtained within lower-order approximations that do not include excitonic correlation (Born approximations). Even though the model is purely fermionic, we have shown how it can be effectively mapped at low temperatures and density to a gas of interacting excitons. We have thus derived an analytical expression for the effective exciton-exciton interaction. The linear optical properties of the system have been calculated including vertex corrections at the Fock level. This ensures the conservation of sum rules in the optical response. The excitonic absorption at low density ensues both in ladder and Born approaches, but the broadenings at the exciton energy are either too small or too large in the Born approximations, depending on whether frequency dependence of the broadening is included or not. Excitonic emission well beyond exciton bleaching is also predicted in all models, but the peak shifts are more pronounced in the Born approximations, showing that a better cancellation between the self-energy and vertex correction results from the introduction of excitons. We have also shown that sizable excitonic gain can be predicted at low temperature and density, when the electron plus hole chemical potential is just below the exciton energy. However, its correct description must include exciton broadening from exciton-exciton scattering, and unphysical values are thus obtained in the Born approximations. These qualitative conclusions clearly hold even for more refined descriptions of the electron-hole plasma than the Born approximations considered here when these descriptions fail to account for excitons in the plasma. This is also the case for the model recently presented by Das Sarma and Wang in Ref. 29, which includes screening at the plasmon-pole approximation level, but no excitons in the electron-hole gas. The excitonic gain calculated using this approximation shows a divergent behavior close to $-E_b$ at appropriate density, which is similar to what we have found for the SCBA. This unphysical result provides a strong experimental test to unvalidate the approach in this particular regime. Also the recent theory by Hannewald *et al.*,[30] while interestingly addressing the nonequilibrium theory of many-body effects in the optical response of the electron-hole system, remains within a nondynamical scheme insufficient to include the existence and formation of bound pairs in the gas.

A last issue concerns the intrinsic limitations of the SCLA. A clear determination of the limits of validity of the SCLA as a function of the strength of the coupling and diluteness of the system is a nontrivial task. To our knowledge the most complete discussion has been provided by Buzatu.[31] In 1D, a direct test of the SCLA (in the case of a contact potential) is possible due to the availability of the exact solution by the Bethe ansatz. Buzatu shows that, in the calculation of the ground state energy, the results obtained using the fermionic ladder approximation can be improved using a simplified self-consistent treatment, and become close to the exact results in a large range of parameters. In the dilute limit he also shows that self-consistent and non-self-consistent results merge and coincide with the exact results. On the other hand, it has been recently demonstrated by Pieri and Strinati[32] using a diagrammatic analysis for 3D systems that, in order to correctly describe the weak residual interaction between excitons in the very dilute limit, ladder diagrams for the composite bosons should be included. Quantitatively, this amounts to an overestimation of the vanishingly small scattering length between excitons in the SCLA. However, we remark that in the present work we have been considering a range of densities and temperatures that places us well above this very dilute limit. This is exemplified in the relevance of free carriers that is expected in this intermediate regime. Clearly, a small parameter for selecting the most relevant diagrams in the self-energy expansion is lacking here, and only comparisons to exact results can establish the real quality of the different approximations.

In conclusion, we have clearly shown that in the definite and important physical region of $T<E_b$ inclusion of excitonic correlation in the electron-hole plasma is relevant and necessary, and that the simplified model presented in this paper is a well-understood starting point for this purpose. Thus, its further developments to address realistic systems in higher dimensions are well motivated.

ACKNOWLEDGMENTS

We thank A. Quattropani, P. Schwendimann, V. Savona, C. Ciuti, and L. J. Sham for stimulating discussions. One of the authors (C.P.) acknowledges support by the Swiss National Foundation for the Scientific Research.

[1] Excellent reviews of the subject may be found in B. I. Halperin and T. M. Rice, in *Solid State Physics*, edited by H. Ehrenreich, F. Seitz, and D. Turnbull (Academic, New York, 1977), Vol. 21; T. M. Rice, *ibid.*, Vol. 32.

[2] H. Haug, Z. Phys. B **24**, 351 (1976).

[3] X. Zhu, M. S. Hybertsen, and P. B. Littlewood, Phys. Rev. B **54**, 13 575 (1996).

[4] R. J. Elliott, Phys. Rev. **108**, 1384 (1957).

[5] H. Haug and S. W. Koch, *Quantum Theory of the Optical and Electronic Properties of Semiconductors* (Singapore, World Scientific, 1990).
[6] H. Haug and S. Schmitt-Rink, Prog. Quantum Electron. **9**, 3 (1984).
[7] W. D. Kraeft, D. Kremp, W. Ebeling, and G. Röpke, *Quantum Statistics of Charged Particle Systems* (Akademie-Verlag, Berlin, 1986).
[8] R. Zimmermann, *Many Particle Theory of Highly Excited Semiconductors* (Teubner, Liepzig, 1988).
[9] M. Pereira and K. Henneberger, Phys. Rev. B **58**, 2064 (1998).
[10] F. Tassone and C. Piermarocchi, Phys. Rev. Lett. **82**, 843 (1999).
[11] S. Benner and H. Haug, Europhys. Lett. **16**, 570 (1991).
[12] F. Tassone and F. Bassani, Phys. Rev. B **51**, 16 973 (1995).
[13] D. G. Mahan, *Many Particle Physics* (Plenum, New York, 1981).
[14] P. Danielewicz, Ann. Phys. (N.Y.) **152**, 239 (1984).
[15] H. Haug and A. P. Jauho, *Quantum Kinetics in Transport and Optical Properties of Semiconductors* (Springer-Verlag, Berlin, 1996).
[16] L. P. Kadanoff and G. Baym, *Quantum Statistical Mechanics* (W. A. Benjamin, Reading, PA, 1962).
[17] R. Cingolani, R. Rinaldi, M. Ferrara, G. C. La Rocca, H. Lage, D. Heitmann, K. Ploog, and H. Kalt, Phys. Rev. B **48**, 14 331 (1993); C. Gréus, A. Forchel, R. Spiegel, F. Faller, S. Benner, and H. Haug, Europhys. Lett. **34**, 213 (1996); R. Ambigapathy, I. Bar-Joseph, D. Y. Oberli, S. Haacke M. J. Brasil, F. Reinhardt, E. Kapon, and B. Deveaud, Phys. Rev. Lett. **78**, 3579 (1997); R. Kumar, A. S. Vengurlekar, A. Venu Gopal, T. Melin, F. Laurelle, B. Etienne, and J. Shah, *ibid.* **81**, 2578 (1998).
[18] G. Baym and L. P. Kadanoff, Phys. Rev. **124**, 287 (1961).
[19] N. E. Bickers, D. J. Scalapino, and S. R. White, Phys. Rev. Lett. **62**, 961 (1989).
[20] B. Kyung, E. G. Klepfish, and P. E. Kornilovitch, Phys. Rev. Lett. **80**, 3109 (1998); M. Y. Kagan, R. Frésard, M. Capezzali, and H. Beck, Phys. Rev. B **57**, 5995 (1998).
[21] R. Haussman, Z. Phys. B: Condens. Matter **91**, 291 (1993).
[22] E. Hanamura and H. Haug, Phys. Rep. **33C**, 209 (1977).
[23] F. Tassone and Y. Yamamoto, Phys. Rev. B **59**, 10 830 (1999).
[24] Y. Nambu, Phys. Rev. **117**, 648 (1960).
[25] M. Lindberg and S. W. Koch, Phys. Rev. B **38**, 3342 (1988).
[26] C. Piermarocchi, R. Ambigapathy, D. Y. Oberli, E. Kapon, B. Deveaud, and F. Tassone, Solid State Commun. **112**, 433 (1999).
[27] J. Ding, H. Jeon, t. Ishihara, M. Hagorott, A. V. Nurmikko, H. Luo, N. Samarth, and J. Furdyna, Phys. Rev. Lett. **69**, 1707 (1992); V. Kozlov, P. Kelkar, A. Vertikov, A. V. Nurmikko, C. C. Chu, J. Han, C. G. Hua, and R. L. Gunshor, Phys. Rev. B **54**, 13 932 (1996).
[28] L. Sirigu, D. Y. Oberli, L. Degiorgi, A. Rudra, and E. Kapon, Phys. Rev. B **61**, R10 575 (2000).
[29] S. Das Sarma and D. W. Wang, Phys. Rev. Lett. **84**, 2010 (2000).
[30] K. Hannewald, S. Glutch, and F. Bechstedt, Phys. Rev. B **62**, 4519 (2000).
[31] F. D. Buzatu, Mod. Phys. Lett. B **9**, 1149 (1995).
[32] P. Pieri and G. C. Strinati, Phys. Rev. B **61**, 15 370 (2000).